THE JOURNAL OF BIOLOGICAL CHEMISTRY VOL. 288, NO. 22, pp. 15988–16003, May 31, 2013

Mechanisms of Neuroprotection from Hypoxia-Ischemia (HI) Brain Injury by Up-regulation of Cytoglobin (CYGB) in a Neonatal Rat Model*

Received for publication, October 17, 2012, and in revised form, April 10, 2013 Published, JBC Papers in Press, April 12, 2013, DOI 10.1074/jbc.M112.428789

Shu-Feng Tian, Han-Hua Yang, Dan-Ping Xiao, Yue-Jun Huang, Gu-Yu He, Hai-Ran Ma, Fang Xia, and Xue-Chuan Shi[1]

From the Department of Pediatrics, the Second Affiliated Hospital, Shantou University Medical College, North Section of Dong-xia Road, Shantou, Guangdong 515041, China

Background: Potential functions of cytoglobin (CYGB) in neonatal hypoxia-ischemia (HI) brain injury have not been reported.
Results: Up-regulation of CYGB reduces HI injury and improves long term cognitive impairment after neonatal HI.
Conclusion: CYGB exhibits neuroprotective effects, possibly through antioxidant and antiapoptotic functions as well as by stimulating angiogenesis.
Significance: These results provide a novel target for developing a clinically relevant strategy for future studies.

This study was designed to investigate the expression profile of CYGB, its potential neuroprotective function, and underlying molecular mechanisms using a model of neonatal hypoxia-ischemia (HI) brain injury. *Cygb* mRNA and protein expression were evaluated within the first 36 h after the HI model was induced using RT-PCR and Western blotting. *Cygb* mRNA expression was increased at 18 h in a time-dependent manner, and its level of protein expression increased progressively in 24 h. To verify the neuroprotective effect of CYGB, a gene transfection technique was employed. *Cygb* cDNA and shRNA delivery adenovirus systems were established (*Cygb*-cDNA-ADV and *Cygb*-shRNA-ADV, respectively) and injected into the brains of 3-day-old rats 4 days before they were induced with HI treatment. Rats from different groups were euthanized 24 h post-HI, and brain samples were harvested. 2,3,5-Triphenyltetrazolium chloride, TUNEL, and Nissl staining indicated that an up-regulation of CYGB resulted in reduced acute brain injury. The superoxide dismutase level was found to be dependent on expression of CYGB. The Morris water maze test in 28-day-old rats demonstrated that CYGB expression was associated with improvement of long term cognitive impairment. Studies also demonstrated that CYGB can up-regulate mRNA and protein levels of VEGF and increase both the density and diameter of the microvessels but inhibits activation of caspase-2 and -3. Thus, this is the first *in vivo* study focusing on the neuroprotective role of CYGB. The reduction of neonatal HI injury by CYGB may be due in part to antioxidant and antiapoptotic mechanisms and by promoting angiogenesis.

Perinatal hypoxia-ischemia (HI)[2] brain injury is a common cause of lifelong morbidities (1, 2). Approximately half of HI events result in death, and 25% of the survivors suffer from neurological disabilities, including cerebral palsy, cognitive and/or sensory deficits, mental retardation, learning disabilities, and epilepsy (3, 4). These impairments significantly impact life experience and social welfare. To date, there are no effective therapies for the treatment of these neurological disorders. Thus, this limitation has provided an incentive to search for new, more effective therapeutic interventions that may lead to better outcomes.

The globins have striking functions, which initially attracted our research interest. Cytoglobin (CYGB), the fourth member of the vertebrate globin family of hemoproteins, is detectable in various organs (5). Hemoglobin and myoglobin are abundant hemoproteins that have been extensively studied. Neuroglobin, the third heme protein (6), can be induced by neuronal hypoxia and cerebral ischemia and can protect neurons from the effects of hypoxia *in vitro* (7, 8) and *in vivo* (8–11). The most recently discovered heme protein, androglobin, the fifth member of globin family, is preferentially expressed in the testis and is insensitive to experimental hypoxia (12). The physiological function of CYGB remains unknown, but it is believed to have various roles due to its family homology, such as storing O_2, facilitating O_2 diffusion, detoxifying reactive oxygen species, acting as an O_2 sensor, and functioning as an NO dioxygenase (5, 13–16). Thus, CYGB may play a cytoprotective role under hypoxic and/or ischemic conditions. Increasing evidence suggests that CYGB may be up-regulated in the liver, heart, brain, muscle, and kidney (16–19) under hypoxic and/or ischemic conditions, suggesting that CYGB might be a protective factor in these organs. Previous studies have also indicated that CYGB acts as a stress-responsive hemoprotein expressed both in the devel-

* This work was supported by Postgraduate Student Training Foundation of Shantou University Medical College Grant LD0504510817. This work was also supported in part by Chinese National Natural Science Foundation for Young Investigators Grant 31140016 and Administration of Science and Technology Research of Guangdong Province, China, Grant 2010B031600282.
[1] To whom correspondence should be addressed. Tel.: 86-754-88915666; Fax: 86-754-88346543; E-mail: shixuechuan@126.com.

[2] The abbreviations used are: HI, hypoxia-ischemia; MWM, Morris water maze; TTC, 2,3,5-triphenyltetrazolium chloride; MDA, malondialdehyde; SOD, superoxide dismutase; ADV, adenovirus; EL, escape latency; P*n*, postnatal day *n*.

oping and adult brain (20) and is protective under oxidative stress in cell lines (21, 22). More recently, *Cygb* was found to act as a tumor suppressor gene (23, 24), and protect kidney fibroblasts under ischemic conditions (25), which are related to oxidative stress (25–27).

Our hypothesis was that CYGB might protect neonatal rats from the damage associated with HI brain injury. The aims of the present study were to investigate the potential role of CYGB in neonatal HI and clarify the underlying mechanisms as well as to provide a new therapeutic target for the treatment of neonatal HI brain injury. For the first time, we identified the expression profiles of *Cygb* mRNA and protein induced by HI using a widely applied animal model. We also provided the first evidence that HI outcomes could be significantly affected under the condition of overexpression and knockdown of *Cygb* using adenovirus transfection systems *in vivo*. MDA and SOD assays were also carried out in order to demonstrate the antioxidant ability of CYGB *in vivo*. In addition, we identified the molecular mechanisms associated with CYGB under HI injury. These findings suggest that CYGB plays an important role in protecting the developing brain against HI injury.

EXPERIMENTAL PROCEDURES

Animals and Experimental Schedule—Sexually mature Sprague-Dawley rats ($n = 28$, male; $n = 56$, female) were purchased from the experimental Animal Center of Shantou University Medical College (Shantou, China). Care of the animals used in this investigation conformed to United States National Institutes of Health guidelines (79) and followed the rules of the National Animal Protection of China. The study was approved by the Institutional Animal Care and Use Committee of Shantou University Medical College. Pregnant females were housed individually, and the presence of pups was checked for daily. The day of birth was considered day 0 (P0), and 1 day later, the litters were culled to 8 rat pups/dam. Animals were maintained in the same temperature- and humidity-controlled holding facility (22–24 °C) under a 12-h/12-h light/dark cycle (light onset at 8:00 a.m.), with free access to food and water. Efforts were made to minimize animal suffering and to reduce the number of animals used. A schedule of the treatment, surgical procedure, and tests of the animals is shown in Fig. 1. 535 neonatal Sprague-Dawley rats were used in this study, and the survival rate of each group (animals used for studying the endogenous expression profiles of *Cygb* and confirming the efficiency of ADV transfection reagents were considered as sham) in the first 36 h after treatment is listed in Fig. 1*C*. Log rank tests were used to compare survival curves among groups at 28 days, when they were ready for the Morris water maze (MWM) test.

Reagents—*In situ* cell death detection kits were purchased from Roche Applied Science. The PCR primers (as listed in Table 1), cDNA, and shRNA for *Cygb* were synthesized by Sangon Biological Engineering Technology and Services Co., Ltd. (Shanghai, China). The RT-PCR kits were purchased from Takara Biotechnology Co., Ltd. (Dalian, China). Rabbit polyclonal antibody for CYGB (FL-190) and goat polyclonal antibody for CD31 were purchased from Santa Cruz Biotechnology, Inc. (Santa Cruz, CA). Primary monoclonal antibody for β-actin, cleaved caspase-2 and -3, and horseradish peroxidase-conjugated secondary antibody were from Cell Signaling Technology, Co., Ltd. The SuperSignal Western blotting detection kits were obtained from Pierce. Cy3-conjugated anti-rabbit secondary antibody and 4′,6-diamidino-2-phenylindole (DAPI) for immunofluorescence were from Sigma-Aldrich. Rabbit anti-VEGF and relative streptavidin peroxidase immunohistochemical staining kits were purchased from Biosynthesis Biotechnology Co., Ltd. (Beijing, China). All surgical materials used were acquired from Yuehua Medical Products Ltd. (Shantou, China). Other chemicals and reagents were of molecular biology grade and were purchased from local commercial stores.

Establishment of Animal Model—HI brain injury was induced in P7 Sprague-Dawley rats based on the classical "Levine method" (28) with modifications by snipping the left common carotid artery between double ligations and prolonging hypoxia duration from 90 min to 120 min. Briefly, each rat was deeply anesthetized by inhalation of isoflurane. The common carotid artery was exposed through a midline cervical incision, permanently double-ligated with 5-0 silk sutures, and severed. The total time for surgery in each animal was ~3 min. After surgery, animals were given 1–2 h to recover from anesthesia. Following recovery, animals were placed in an airtight container partially submerged in a 37 °C water bath to maintain a constant thermal environment. A 120-min continuous hypoxia (8% O_2, 92% N_2) was used to induce systemic hypoxia. Sham animals received anesthesia and exposure of the left common carotid artery but did not receive HI treatment. After another 30-min recovery, all surviving rats were returned to their cages and kept in a standard environment as described under "Animals and Experimental Schedule."

Construction of Adenovirus-mediated Transfection Systems—shRNA and cDNA of *Cygb* sequences were designed based on a protocol used in a previous study (23). We obtained plasmids PDC316-mCMV-Zsgreen-cDNA-*Cygb* and PDC316-Zs-Green-shRNA-*Cygb*, with null vectors transfected as negative controls (29–32). The plasmids were cloned to adenovirus vectors, and the viral null vectors were propagated in human embryonic kidney 293 (HEK 293) cells. Viral titer was determined by using standard plaque assays on HEK293 cells. The resulting titers for *Cygb*-shRNA-ADV and *Cygb*-cDNA-ADV were 3×10^9 and 2×10^9 pfu/ml, respectively.

Intracerebroventricular Injection of Adenovirus—Adenoviral vectors delivery were conducted on P3 Sprague-Dawley rats based on protocols described previously (29, 33). Briefly, the rats were anesthetized with isoflurane and mounted onto an SR-6N stereotactic frame (Narishige Scientific Instrument Laboratory, Tokyo, Japan). 4 μl of adenoviral vectors or saline (NaCl solution) were injected into the lateral ventricle (0.8 mm posterior and 1.0 mm lateral in relation to λ and at a depth of 3 mm from the skin surface of the brain) (33) using a Hamilton syringe with a 10-gauge needle. The vector or saline was injected over a period of 2 min, and the needle was left in place for another 2 min and then removed slowly over 2 min. In order to avoid the potential effect of tissue damage caused by the injection procedure on the assessment of HI injury, all injections were made into the cerebral ventricle contralateral to the injury hemisphere.

TABLE 1
Primer sequences for PCR amplification

Gene name (ID)	Sequences	Product size
		bp
***Cygb* (NM_130744.2)**		
Forward	5′-CCTGGTGAGGTTCTTTGTGAAC-3′	262
Reverse	5′-CAGAATGACCCCAGAGAGAATC-3′	
***Hif-1α* (NM_024359.1)**		
Forward	5′-TCCATTACCTGCCTCTGAAACT-3′	294
Reverse	5′-GGATTCTTCGCTTCTGTGTCTT-3′	
Caspase-2 (NM_022522.2)		
Forward	5′-GAGCAATGTGCACTTCACTGG-3′	224
Reverse	5′-CCACACCATGTGAGAGGAGTG-3′	
Caspase-3 (NM_012922.2)		
Forward	5′-GGAGCAGTTTTGTGTGTGTGAT-3′	200
Reverse	5′-TCCACTGTCTGTCTCAATACCG-3′	
***Vegf* (NM_031836.2)**		
Forward	5′-CGGACAGACAGACAGACACC-3′	175
Reverse	5′-CCCAGAAGTTGGACGAAAAG-3′	
β-Actin (NM_031144.2)		
Forward	5′-ACCCTGAAGTACCCCATTG-3′	247
Reverse	5′-TACGACCAGAGGCATACAG-3′	

To confirm adenovirus-mediated expression *in vivo*, ADV vectors were tagged with green fluorescence protein (GFP), and expression was detected using a Zeiss Axio Imager Z1 inverted microscope 4 days postinjection. To evaluate temporal change of the expression of CYGB protein after transfection, rats were euthanized at 1, 3, 5, and 7 days after injection of the vectors ($n = 3$), and the cortex and hippocampus were harvested for Western blot analysis.

Immunofluorescence—Neonatal rats were sacrificed 4 days after saline or ADV vector injection. Three rats were used for each group, and three sham rats were used as control. Targeted brain tissues (3–4 mm) were obtained as indicated in Fig. 1*B* and then fixed for 18 h in 4% paraformaldehyde in PBS at 4 °C, followed by incubation in 30% sucrose in PBS overnight at 4 °C. Then the fresh brain tissues were embedded in O.C.T and cut into 25-μm-thick sections using a cryostat, and the sections were mounted onto glass slides and stored at −80 °C. The brain sections were fixed with precooled acetone for 15 min at 4 °C and rinsed with PBS for 5 min. The sections were then incubated in PBS buffer containing 0.1% Triton X-100 for 15 min and then blocked with 5% BSA in PBS. Blocked sections were then treated overnight with primary antibody at 4 °C. The primary antibody used was rabbit anti-CYGB diluted (1:100) in PBS containing 1% BSA. The sections were rinsed with washing buffer and then incubated in secondary antibody for 1 h at room temperature in the dark. The secondary antibody used was Cy3-conjugated goat anti-rabbit IgG (1:1000). Samples were washed and stained by DAPI for 10 min at room temperature in the dark and then washed again, mounted with glycerol/PBS, and observed using a Zeiss Axio Imager Z1 inverted microscope.

RT-PCR—Total RNA was prepared from samples of injured tissues (Fig. 1*B*) using TRIzol reagent (Invitrogen), following the manufacturer's instructions. After establishing HI for the 0, 6, 12, 18, 24, and 36 h time points, rats from different groups were euthanized. RT-PCR experiments and analysis of results were performed as described previously (34) to evaluate the mRNA expression pattern of *Cygb* under HI conditions. Then we conducted HI treatment within specific time windows (the time for reaching the peak of endogenous *Cygb* mRNA up-regulation) to rats that had been given saline, ADV only, shRNA, or cDNA treatment to reveal expression of the potential candidates, including *Hif-1α* (hypoxia-inducible factor 1α) *Vegf*, caspase-2, and caspase-3. The sham group served as control. The PCR primers used are shown in Table 1. β-Actin was used in each assay to normalize the amount of mRNA.

Western Blotting—To evaluate changes of endogenous expression of CYGB after HI injury, rats were euthanized at 0, 6, 12, 18, 24, and 36 h, and the injured hemisphere of the brain (~100 mg; indicated in Fig. 1*B*) was collected. In addition, as mentioned previously, rats were euthanized at 1, 3, 5, and 7 days after receiving an injection of the *Cygb*-shRNA or *Cygb*-cDNA vectors. P7 rats (4 days after injection) injected with the ADV vector only or with saline served as the ADV vector only group and control group. Brain tissues were homogenized in cold radioimmune precipitation assay lysis buffer (Beyotime, Jiangsu, China), and the protein concentrations were determined by BCA assay kits (Beyotime). Equal amounts of protein (40 μg) were separated on 12% SDS-PAGE and transferred onto a polyvinylidene fluoride (PVDF) membrane (pore size, 0.22 μm; Millipore). The membrane was blocked by a 1-h incubation at room temperature in a Tris-buffered saline solution (TBS-T; 20 mM Tris, pH 7.6, 135 mM NaCl, and 0.05% Tween) containing 5% nonfat dry milk and then incubated with different primary antibodies, including anti-CYGB (1:400 dilution; Santa Cruz Biotechnology, Inc.), anti-β-actin (1:1000 dilution; CST) overnight at 4 °C. After washing the membrane three times with TBS-T, the secondary antibody HRP-labeled goat anti-rabbit IgG was then added to the membrane according to the vendor's recommendation (1:8000 dilution; CST) and incubated for 1 h at room temperature and then washed again as described previously. The bound antibodies were detected by using SuperSignal Western blotting kits. Quantity One software (version 4.5.2; Bio-Rad) was used to perform densitometric analysis of Western blots. The expression of β-actin was used as a control for equal protein loading.

To reveal the association between caspase activation and CYGB expression, we conducted HI treatment at specific time

windows (the time for reaching the peak of endogenous CYGB protein up-regulation) to rats that had been given saline, ADV only, shRNA, or cDNA treatment. The sham group served as a control. Samples were harvested at the time point that demonstrated the highest transfection efficiency, which was 24 h post-HI in this study. The activation levels of both cleaved caspase-2 and cleaved caspase-3 were studied following the steps described above. The conditions of primary antibodies used were as follows: anti-cleaved caspase-2 (1:1000) and anti-cleaved caspase-3 (1:1000).

2,3,5-Triphenyltetrazolium Chloride (TTC) Staining—As described previously (35), 24 h after HI induction, TTC staining was performed ($n = 8$) to measure the infarct volume. The animals were perfused transcardially with cold saline under deep anesthesia, and brains were quickly removed and subsequently embedded in brain matrix and frozen for 3 min at −80 °C. Each brain was sliced coronally at 2-mm intervals with the matrix. Four sliced sections were then subsequently stained with 1% TTC (w/v) at 37 °C for 12 min and then fixed in 4% (w/v) formaldehyde in PBS for 24 h at 4 °C. Finally, the brain slice images were captured using a digital camera (SONY DSC-W150), and the areas of unstained tissue (the infarct areas) were delineated manually using Image Pro Plus, version 6.0, software by a person blinded to the treatment groups. The corrected infarct area was calculated as the total area of the infarct area minus the edema area (calculated as the ischemic hemisphere area minus the contralateral hemisphere area). The corrected infarct volume was then calculated by the sum of the corrected infarct area on each section multiplied by slice thickness. Total corrected infarct volume was expressed as a percentage of the contralateral hemisphere area. Because this kind of data is usually binomially distributed, an arcsine transformation that can be calculated by using the formula, $x = \text{arcsine}\ \sqrt{p}$, should be done in the statistical software first before further analysis.

Nissl Staining—The targeted brain specimens (Fig. 1*B*) obtained 24 h after HI were fixed in 4% (w/v) formaldehyde in PBS, paraffin-embedded, and sliced in sections of 3-μm thickness. For Nissl staining ($n = 8$), after dewaxing in xylene and rehydration through graded ethanol, the sections were hydrated in 1% (w/v) toluidine blue at 37 °C for 20 min. After rinsing with double-distilled water, they were dehydrated and mounted with Permount. Eight slices per brain were used for cell counting. Six fields of each slice in the injured side both of the cerebral cortex and hippocampus (CA1) were chosen randomly at ×400 magnification to count staining cells. Imaging-Pro-Plus software, version 6.0, was used to perform quantitative analysis of cell number counts. The mean number of intact neurons in the six views was used for cell counts in each section. The final average number of the eight sections from each sample was used for analysis.

TUNEL Staining—TUNEL staining ($n = 8$) was performed on paraffin-embedded sections by using the *in situ* cell death detection kit, according to the manufacturer's instructions. Briefly, sections were deparaffinized in xylene, rehydrated through graded ethanol, rinsed in 3% hydrogen peroxide, and treated with proteinase K (20 mg/ml) for 25 min at room temperature. Subsequently, the sections were incubated with the TUNEL reaction mixture for 1 h at 37 °C. After washing with PBS, the sections were incubated with Converter-POD for 30 min and then visualized with 3,3′-diaminobenzidine. Sections were then counterstained with hematoxylin for 3 min and rinsed under running water. After dehydration in graded ethanol series and being rendered transparent in xylene, the brain sections were mounted onto gelatin-coated slides. Apoptotic cell counting was performed in the hippocampus (CA1) and cerebral cortex in the hemisphere that was ipsilateral to the injured hemisphere. Cells with yellow-brown granules in the nucleus were considered to be apoptotic cells. In evaluating numeric density, total TUNEL-positive stained neurons were calculated in six views under the light microscope with ×400 magnifications. The mean number of apoptotic neurons was used for cell counts in each section. The final average number of apoptotic neurons of eight sections from each sample was used for analysis, and the severity of brain damage was evaluated by the apoptotic index, defined as the average number of TUNEL-positive neurons.

Histology and Immunohistochemistry—Four paraffin sections from each sample ($n = 8$) from the sham, HI, shRNA, and cDNA groups were processed for hematoxylin and eosin (HE) for the examination of brain tissue under light microscopy. For VEGF and CD31 staining, briefly, after deparaffinization and redehydration, nonspecific endogenous peroxidase activity was blocked by treating sections with 3% hydrogen peroxide in methanol for 25 min. The antigen was recovered by boiling the sections for 15 min in 10 mM citrate buffer (pH 6.0). Nonspecific binding was blocked with 1% non-immune serum in PBS for 30 min. The sections were then incubated with anti-VEGF (1:300) or anti-CD31 (to stain endothelial cells) (1:60) overnight at 4 °C. They were then washed with PBS, incubated with a biotinylated goat anti-rabbit IgG (1:300) for 1 h at 37 °C, washed, and incubated with an avidin peroxidase conjugate solution (1:100) for 1 h. Finally, the sections were developed with diaminobenzidine for 5 min. Negative controls were similarly processed without the primary antibody. Five slides from each brain, with each slide containing six fields, were digitized under ×100 magnifications by two independent observers who were blinded to the experimental conditions. The density and size of the vasculature were analyzed in a blinded manner in digital images using the Imaging-Pro-Plus software, version 6.0.

MDA and SOD Assays—Brain samples were taken from the injured hemispheres of rats at 24 h after hypoxia-ischemia induction ($n = 8$). The MDA level and SOD activity were measured according to the manufacturer's specifications (Beyotime). Briefly, the tissues were homogenized and centrifuged at 2000 × *g* for 10 min at 4 °C. The supernatant was collected to measure the MDA level and SOD activity. The protein content of the supernatant was measured as described under "Western Blotting." The MDA level and SOD activity were measured using the thiobarbituric acid and xanthine oxidase methods. The absorbance levels of the MDA and SOD test samples were measured using a spectrophotometer (Thermo) at 532 and 550 nm. The MDA levels and SOD activities were expressed as nmol/mg protein and units/mg protein.

Morris Water Maze Test—Spatial learning and memory abilities were evaluated using the MWM test with P28–P33 rats ($n = 8$) (36). A circular pool (160-cm diameter × 50-cm high)

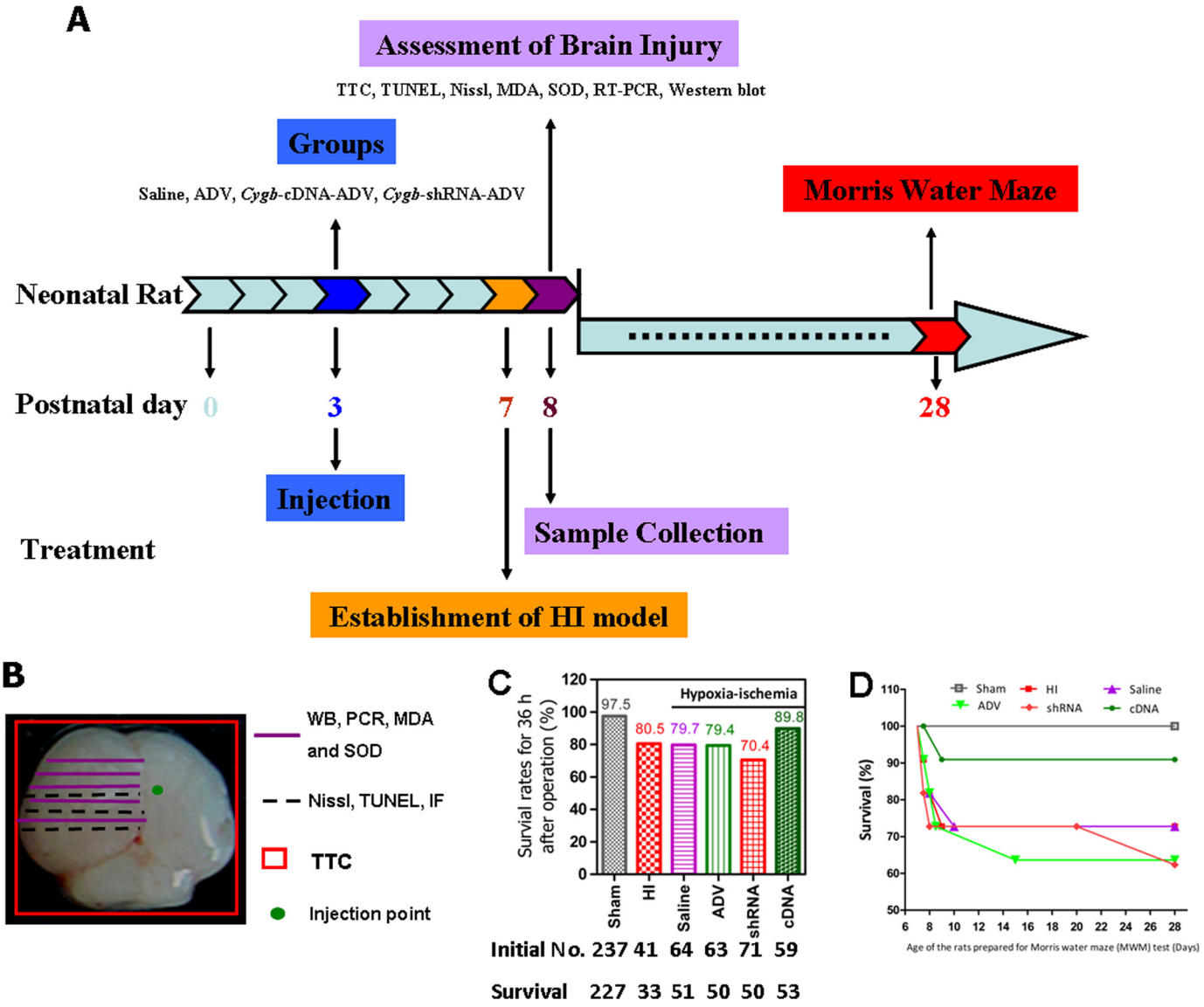

FIGURE 1. *A*, schedule for the treatment, surgical procedure, and experimental tests. Neonatal rats at day 3 were randomly divided into saline, ADV only, *Cygb*-cDNA-ADV, and *Cygb*-shRNA-ADV groups before injections. After evaluating temporal change of the expression of CYGB protein preliminarily at 1, 3, 5, and 7 days after vector injection, we identified day 5 as the best time point for assessing the outcomes affected by the expression of CYGB. Then we induced the HI model in the 7-day-old neonatal rats. 24 h later, brain tissue was harvested. Western blotting, RT-PCR, TTC, TUNEL, Nissl, MDA, and SOD assays were carried out. Long term spatial learning and memory abilities were assessed from day 28 to day 33. *B*, corresponding experiments were conducted in the indicated regions of neonatal brain. The *green round point* indicates the location of the injection. RT-PCR and Western blotting (*WB*) quantitative analysis was conducted using coronal sections of left brain tissues between 3 mm before and 3 mm behind the injection point in order to measure *Cygb* mRNA and protein expression (the same area was used for MDA and SOD assays). Brain tissue (including both of cortex and hippocampus areas, ~3–4 mm) was used for Nissl, TUNEL staining, and immunofluorescence examination. Whole brain was used for TTC staining to detect the infarct. *C*, survival rates of neonatal rats from different groups 36 h after operation (sham or HI treatment). In addition, the *survival curves* are displayed for rats that were assessed in the MWM test at 28 days (*D*).

divided into four quadrants was filled with water (22 ± 1 °C), and a 12 × 12-cm platform was positioned 1 cm below the water surface in the center of one of the quadrants. Four points on the perimeter of the pool were designated, and room lights illuminated the pool. The swimming path of the rats was recorded using a video camera mounted above the center of the pool and analyzed using a video tracking and analysis system (Institute of Materia Medica, Chinese Academy of Medical Sciences). On each training day (P28–P32), the rats received eight consecutive training trials, during which the hidden platform was kept in a constant location. A different start location was used on each trial, which consisted of a search followed by a 20-s platform sit. The time to reach the platform was recorded. If a rat could not find the platform within 90 s, it was led to the platform by the experimenter for a 20-s rest. On the fifth day (P33), memory retention was evaluated during a 90-s probe trial carried out 24 h after the last training session in the absence of the escape platform. The test parameters included time to reach the platform, swimming track, swimming distance of the platform space, and traversing times of the platform.

Statistical Analysis—Each experiment was performed at least three times. Statistical analysis was performed using GraphPad Prism software, version 5.01 (San Diego, CA). Continuous data were expressed as mean ± S.D. One-way analysis

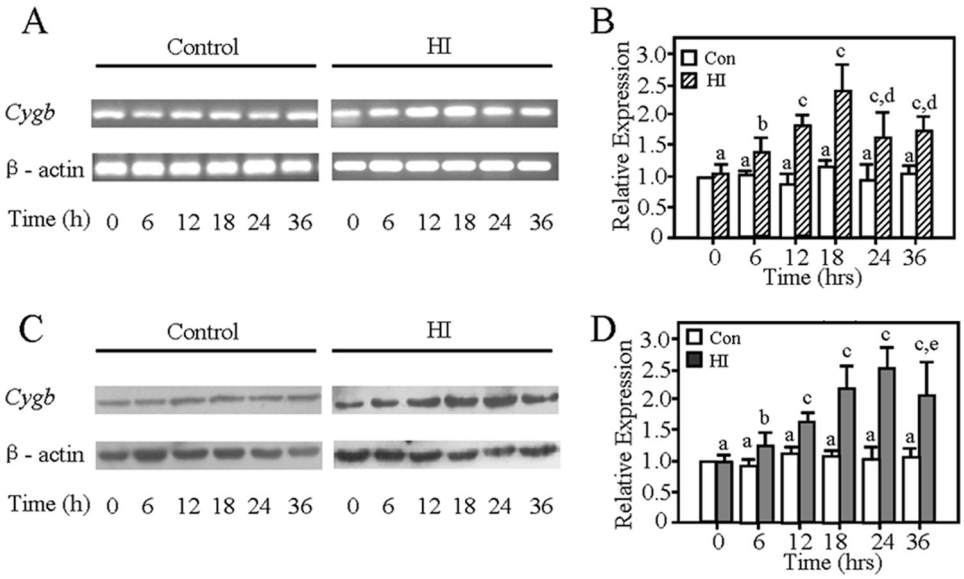

FIGURE 2. **Both mRNA and protein expression profiles of *Cygb* within 36 h after neonatal rats suffered from HI.** *Cygb* mRNA increased in a time-dependent manner in 18 h (*A* and *B*). C, representative electrophoretic image of the study on CYGB protein induced by HI. The results show that CYGB protein levels increased in 6 h, peaking at 24 h post-HI (*D*). Results are presented as mean ± S.D. (*error bars*) in triplicate independent experiments ($n = 3$). *a*, no significant difference as compared with the control group at 0 h. *b*, $p < 0.05$; *c*, $p < 0.01$ as compared with control group at the same time. *d*, $p < 0.05$ as compared with the HI group at 18 h. *e*, $p < 0.05$ as compared with the HI group at 24 h.

of variance followed by Student-Newman-Keuls test was used to compare the differences among multiple groups. Log rank tests were done to compare the survival curves among groups. Data from Morris Water Maze tests were analyzed using the general linear models with repeated measures analysis of variance. A probability (*p*) value less than 0.05 was regarded as statistically significant.

RESULTS

Survival—In this study, 535 neonatal rats were used, and the total survival rate of animals was 87.4%. The survival rate of pups appeared unaffected by pretreatment before HI, indicating that vehicle injection did not significantly affect their survival. The survival rates among HI, saline-HI, and ADV-HI groups were not significantly different (Fig. 1*C*) 36 h after HI induction. However, the survival rate of the *Cygb*-shRNA-ADV-HI group was 70.4%, whereas the *Cygb*-cDNA-ADV-HI group was 89.8%. This indicated that overexpression of *Cygb* increased the survival rate of animals, whereas inhibition of *Cygb* expression decreased survival. In addition, the 28-day survival curves also showed a consistent result (Fig. 1*D*). Overexpression of *Cygb* improved the survival of rats suffering from HI.

Cygb Is Induced by HI in Vivo—We evaluated the changes of endogenous *Cygb* expression in the brain after HI in the P7 rat pups (Fig. 2). *Cygb* mRNA levels were measured by RT-PCR at the 0, 6, 12, 18, 24, and 36 h time points after HI. As shown, the transcriptional level of *Cygb* increased in a time-dependent manner 18 h after HI (Fig. 2, *A* and *B*). The protein level of CYGB was detected by Western blotting at 0, 6, 12, 18, 24, and 36 h after HI. Endogenous CYGB expression in the ipsilateral hemisphere significantly increased from the 6 h time point post-HI and gradually peaked at 24 h after HI (Fig. 2, *C* and *D*). CYGB was elevated nearly 3-fold as compared with sham group at the 24 h time point. Therefore, CYGB may be involved in the pathogenesis process of HI.

Adenovirus-mediated Transfection Alters Expression of CYGB in Vivo—ADV vectors were tagged with GFP, and expression was measured in the periventricular area (Fig. 3*E*). CYGB protein level was detected on days 1, 3, 5, and 7 after injection in P3 rats (Fig. 3, *A–D*). Expression of CYGB peaked at 5 days postinjection (Fig. 3, *B* and *D*). In order to further assess whether the transfection systems were down-regulated or up-regulated, CYGB expression was examined in the region of interest, using immunofluorescence co-localization analysis 4 days after saline or ADV vector injection (Fig. 3*F*). Although the subcellular distribution of CYGB was not thoroughly assessed, we found that CYGB was localized in both the cytoplasm and nuclei of hippocampus neurons (Fig. 3*F*), a finding that is consistent with the distribution pattern reported previously (15). The results showed that *Cygb*-shRNA-ADV and *Cygb*-cDNA-ADV exhibited significant effects in regulating CYGB expression of the brain, which is consistent with the Western blotting data (Fig. 3, *A–D*). Results from the saline or ADV only group indicated that there was no effect on CYGB expression. Together with these results and the expression profiles of *Cygb* mRNA and protein shown above, the animal HI model was induced at day 4 postinjection for subsequent assays in this study.

Adenovirus-mediated Transfection Alters the Expression of Cygb in the Developing Brain 24 h Post-HI—To confirm how different levels of *Cygb* expression affect the outcomes of neonatal HI brain damage, we assessed the *Cygb* mRNA and protein levels in developing brain tissues from different groups 18 or 24 h post-HI. Western blotting revealed that CYGB protein expression was significantly lower in the *Cygb*-shRNA-ADV group as compared with the sham, ADV only, and saline

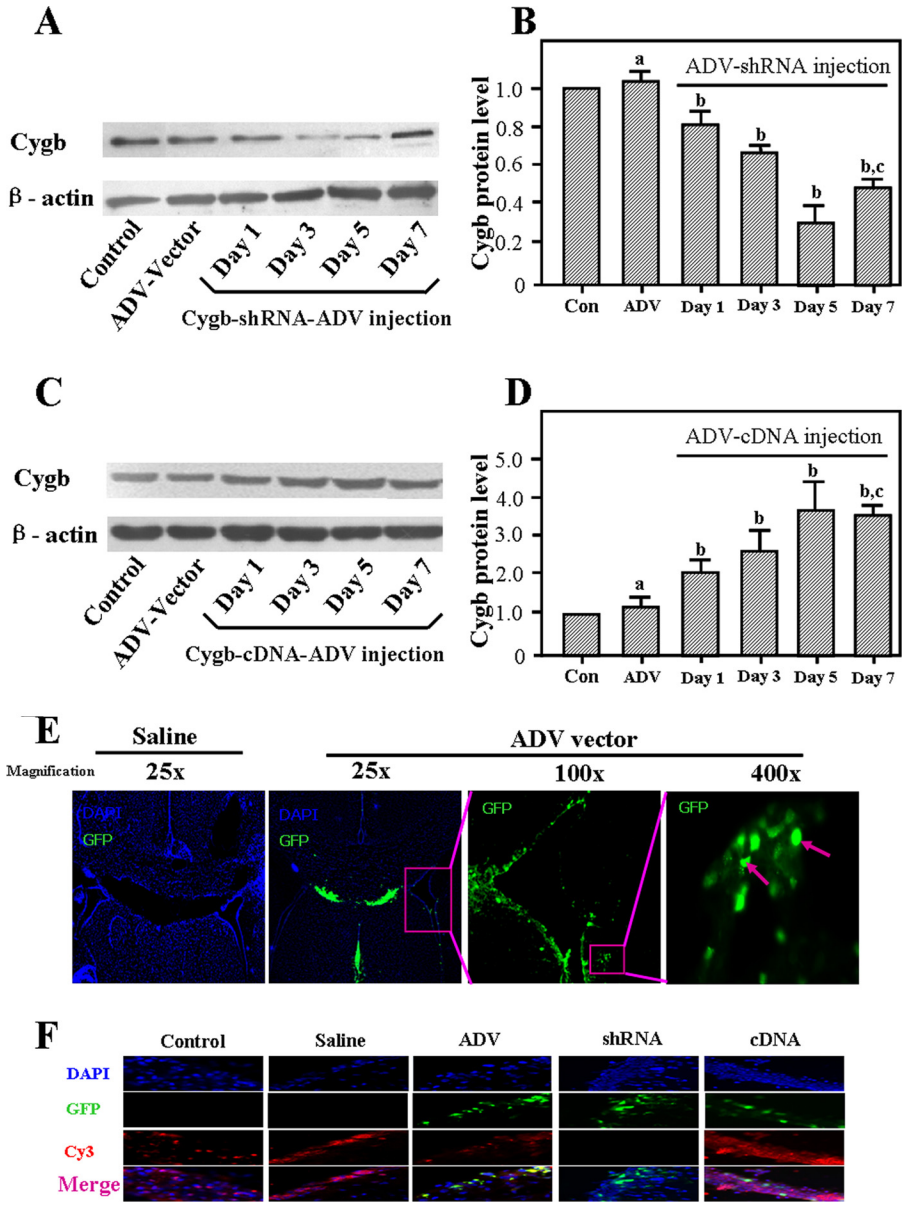

FIGURE 3. **Infection of neonatal brain with adenovirus carrying *Cygb* cDNA or shRNA.** CYGB expression at various time points was confirmed by Western blotting using anti-CYGB antibody. β-actin was used as an internal control. *A* and *C*, representative electrophoretic images. The results showed that 5 days postinjection, inhibition and overexpression of CYGB reached their peaks (*B* and *D*). The ADV-null vector did not affect the expression of CYGB. The data are expressed as mean ± S.D. (*error bars*) in triplicate independent experiments ($n = 3$ per time point per group). *a*, no significant difference; *b*, $p < 0.01$ as compared with control group; *c*, $p < 0.05$ as compared with the 5-day postinjection group. GFP could be detected in the periventricular area in the ADV system group (*E*). Intense GFP (*green color*) signals could be observed in the brain of ADV group at 4 days after ADV vector administration, but there was no GFP-positive signal detected in the saline group. The *pink arrows* point to ADV-transfected cells. The original magnifications are shown. *F*, images of GFP (*green color*), DAPI-stained nuclei (blue color), and CYGB-positive signals (*red color*; Cy3) for the hippocampus (near left lateral ventricle) are depicted 4 days after injection under normal conditions ($n = 3$). Corresponding *merged images* are also shown. The results are consistent with the Western blotting data described above. Original magnification was ×400.

groups, and expression levels were higher in the *Cygb*-cDNA-ADV group as compared with sham group (Fig. 4, *B* and *D*). In addition, RT-PCR analysis also exhibited that *Cygb*-shRNA-ADV inhibited *Cygb* mRNA expression, whereas *Cygb*-cDNA-ADV enhanced its expression as compared with ADV only or saline groups 18 h post-HI (Fig. 4, *A* and *C*). As compared with the sham group, expression levels of CYGB in HI-ADV and HI-saline groups were significantly higher, indicating that HI could induce *Cygb* expression (Fig. 4, *A–D*). Together, these data show that *Cygb* expression was mediated by exogenous *Cygb*-cDNA-ADV and *Cygb*-shRNA-ADV despite endogenous up-regulation in the neonatal HI model.

CYGB Reduces Injury in the Neonatal HI Model—Rats from different groups were sacrificed 24 h post-HI, and morphological injury was assessed by TTC, Nissl, and TUNEL staining. Fig. 5 shows images of neonatal rat brain.

Quantitative assessment of TTC-stained sections was used to assess brain infarct volume in different groups (Fig. 5*A*). Our findings showed that injection with *Cygb*-shRNA-ADV dramatically increased the infarct volume at 24 h after HI injury

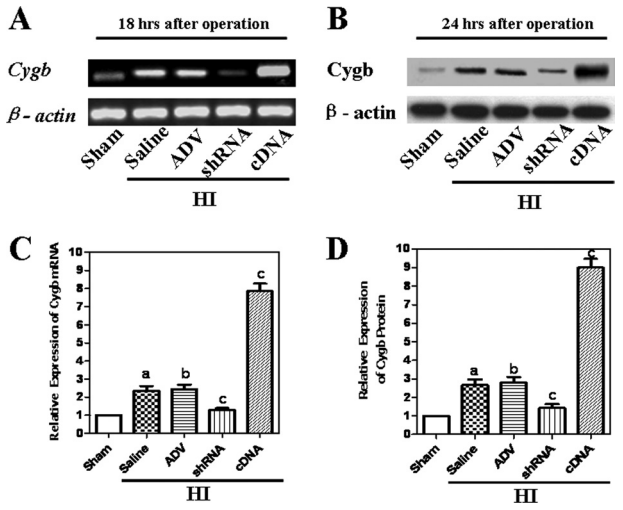

FIGURE 4. **The expression of *Cygb* in HI animals injected with shRNA or cDNA.** The expression of *Cygb* mRNA at 18 h post-HI was confirmed by RT-PCR (*A*). The expression of CYGB protein at 24 h post-HI was confirmed by Western blotting using anti-CYGB antibody (*C*). β-Actin was used as an internal control. The expression levels of CYGB in the sham group were normalized to 1.0. The data are expressed as mean ± S.D. (*error bars*) in triplicate independent experiments ($n = 3$). The results show endogenous up-regulation of CYGB in rats exposed to HI, and both mRNA and protein levels of CYGB were inhibited by shRNA but enhanced by cDNA at 18 h and 24 h, respectively (*B* and *D*). The ADV-null vector did not affect the expression of *Cygb*. *a*, $p < 0.01$ as compared with the sham group; *b*, no significant difference as compared with the saline group; *c*, $p < 0.01$ as compared with the saline group.

($p < 0.01$) (Fig. 5*B*). Injection with *Cygb*-cDNA-ADV resulted in a significant decrease in brain infarct volume as compared with the ADV only group or the saline group ($p < 0.01$). There was no difference between saline, ADV only pretreatments, and untreated HI group, yet all HI groups with or without preinjection of different reagents were significantly different as compared with the sham control group ($p < 0.05$).

Neuronal cell loss in both the ipsilateral cortex and hippocampus was identified by Nissl staining 24 h post-HI injury (Fig. 5*C*). As expected, HI significantly reduced the number of cells and resulted in smaller and irregularly arranged neurons in the brain 24 h after HI as compared with the contralateral part or the sham control group (Fig. 5*E*). Furthermore, inhibition of *Cygb* significantly reduced the number of neuronal cells under HI as compared with the saline- or ADV only-pretreated group ($p < 0.01$). However, more Nissl-stained cells were observed in the *Cygb* overexpression group than in the other HI group ($p < 0.01$).

TUNEL staining of tissue sections was carried out to determine if CYGB could prevent apoptosis at an acute stage of neonatal HI injury. Significantly more apoptotic cells were observed in the *Cygb*-shRNA-ADV group compared with control HI groups 24 h post-HI ($p < 0.01$; Fig. 5, *D* and *F*); however, the number of cells was significantly lower in the *Cygb*-cDNA-ADV treatment group ($p < 0.01$). There was no significant difference in the number of TUNEL-positive cells in the cortex and hippocampus across three control HI groups, whereas HI induced a greater number of apoptotic neurons as compared with the sham group ($p < 0.05$).

CYGB Exhibits Antioxidant Action in the HI Model—To evaluate the antioxidant activity of CYGB, we measured the MDA level and SOD activity 24 h after HI insult ($n = 8$). These findings indicate that inhibition of *Cygb* significantly increased MDA levels and decreased SOD activity, whereas *Cygb* overexpression significantly decreased MDA levels and increased SOD activity as compared with the HI group ($p < 0.01$; Fig. 6*A*). There was no difference between HI, HI-saline, and HI-ADV groups, although all three groups demonstrated increased MDA levels and decreased SOD activity as compared with the sham group ($p < 0.01$).

CYGB Plays a Critical Role in Antiapoptosis and Promotes Angiogenesis—Transcriptional levels of caspase-2, caspase-3, *Hif-1α*, and *Vegf* in HI brain tissue ($n = 3$) were measured by RT-PCR 18 h after HI in three different groups (HI, HI-*Cygb*-shRNA-ADV, and HI-*Cygb*-cDNA-ADV; Fig. 6, *B* and *C*). *Cygb* was inhibited by *Cygb*-shRNA-ADV but enhanced by *Cygb*-cDNA-ADV (Fig. 6*B*). *Hif-1α* and *Vegf* are protective factors in HI, whereas caspase-2 and -3 play an important role in apoptotic pathways. In the present study, we found that *Cygb*-cDNA-ADV could induce *Vegf* mRNA expression but inhibit caspase-2 and -3 mRNA levels as compared with the HI groups ($p < 0.01$; Fig. 6*C*). These results are consistent with previous studies (37–39) and suggest that these three factors are critical for understanding the mechanism underlying the neuroprotective effect of CYGB in neonatal HI.

Furthermore, to confirm whether the effect of *Cygb* overexpression/knockdown on *Vegf*, caspase-2, and caspase-3 is specific to HI conditions, we conducted a RT-PCR assay. RNA was extracted from samples harvested 5 days after *Cygb*-shRNA-ADV and *Cygb*-cDNA-ADV injection (Fig. 6*D*). The results indicated that *Cygb* expression did not significantly affect the expression of these three genes under basal conditions (Fig. 6*E*).

HE staining revealed that cell morphology and microvessels were disrupted (Fig. 6*F*), and immunostaining indicated that higher levels of VEGF protein were expressed in the *Cygb* overexpression group (Fig. 6, *G* and *H*). Immunohistochemical staining of CD31 revealed that a smaller number of microvessels were distributed in the shRNA group, whereas more microvessels were distributed in the cDNA group compared with the HI group (Fig. 6, *I* and *J*), similar to the number of microvessels with a diameter larger than 15 μm/section (Fig. 6, *I* and *K*).

Western blotting showed that both HI-induced cleaved caspase-2 and cleaved caspase-3 were decreased by *Cygb* overexpression, whereas they were increased in the *Cygb* knockdown (Fig. 7, *A*–*C*). There was no significant difference between the *Cygb*-shRNA-ADV and *Cygb*-cDNA-ADV groups in *Hif-1α* mRNA expression levels (Fig. 6*C*). Thus, we propose that *Hif-1α* may be the upstream factor promoting *Cygb* expression, similar to neuroglobin (40), and *Vegf*, caspase-2, and caspase-3 are downstream target genes of *Cygb*.

CYGB Improves Long Term Learning and Memory in the HI Model—The Morris water maze test ($n = 8$) was performed at 3 weeks post-HI (P28 rats) to evaluate long term spatial learning and memory abilities dependent upon the function of the hippocampus and cortex (41). The escape latency (EL) in training days (P28–P32) is shown in Fig. 8*A*. The results showed longer EL in the HI group as compared with the sham group ($p < 0.01$). EL in the *Cygb*-shRNA-ADV group was significantly longer compared with HI group ($p < 0.01$), whereas *Cygb*-cDNA-ADV

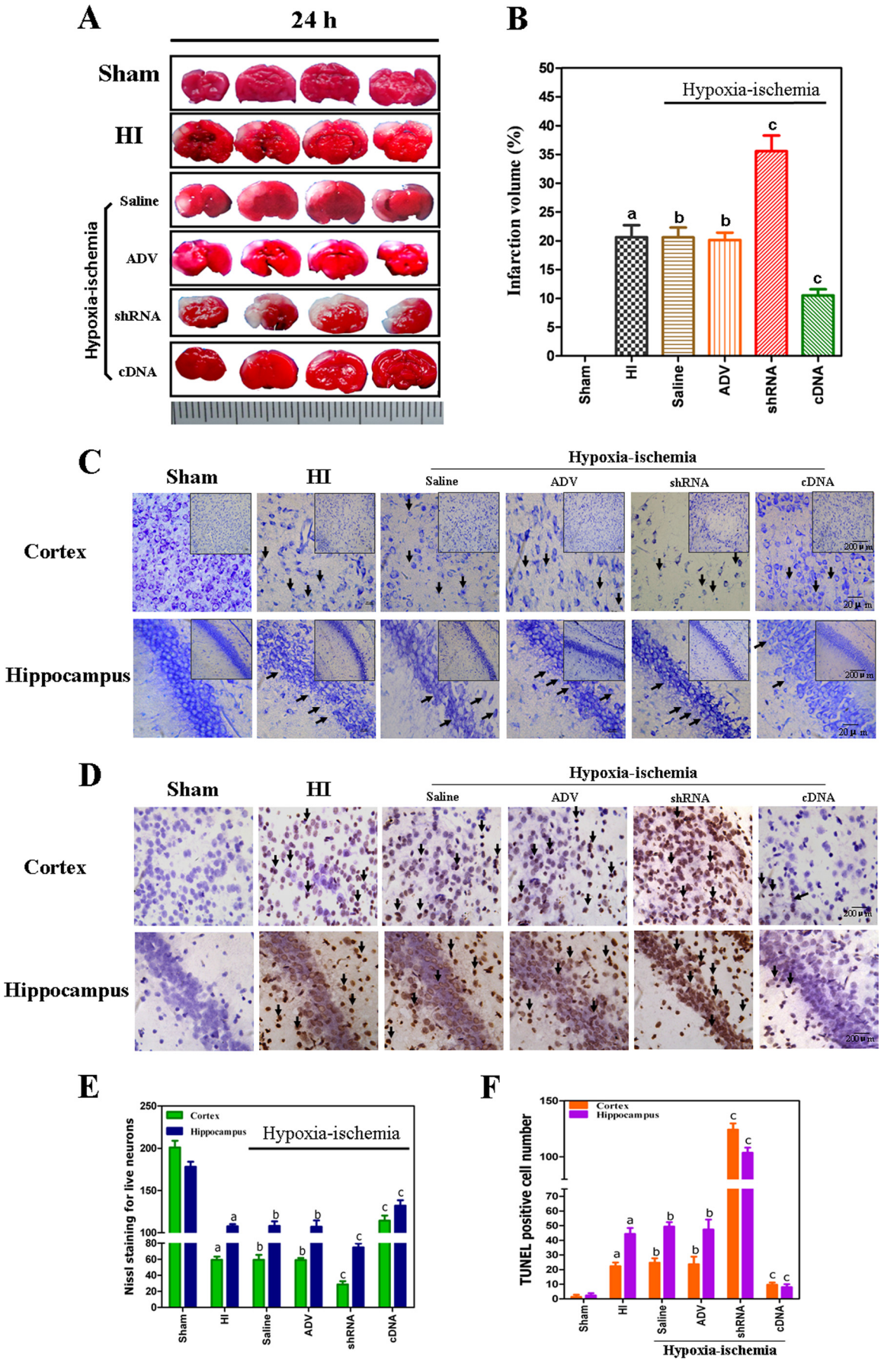
A
24 h
Sham
HI
Hypoxia-ischemia
Saline
ADV
shRNA
cDNA
B
Hypoxia-ischemia
Infarction volume (%)
Sham
HI
Saline
ADV
shRNA
cDNA
C
Sham
HI
Hypoxia-ischemia
Saline
ADV
shRNA
cDNA
Cortex
Hippocampus
200 μm
20 μm
D
Sham
HI
Hypoxia-ischemia
Saline
ADV
shRNA
cDNA
Cortex
Hippocampus
200 μm
E
Cortex
Hippocampus
Hypoxia-ischemia
Nissl staining for live neurons
F
Cortex
Hippocampus
TUNEL positive cell number
Hypoxia-ischemia

groups had significantly shorter EL ($p < 0.01$). There was no significant difference in EL between the HI, saline, and ADV only groups. The space probe trial was conducted after spatial maze training. Platform crossing times and the time spent in the target quadrant were also recorded (Fig. 8, *B* and *C*). Animals in the sham group had a crossing frequency of ~10 times, whereas the HI, saline, and ADV groups had about a crossing frequency of 3 times, and there was no significant difference among these three groups (Fig. 8*B*). The crossing frequency was reduced to twice in the *Cygb*-shRNA-ADV group. In contrast, *Cygb*-cDNA-ADV significantly increased the crossing frequency. HI rats spent less time in the target quadrant compared with sham rats ($p < 0.01$), and *Cygb* inhibition significantly reduced time spent in the target quadrant compared with HI rats ($p < 0.01$; Fig. 8*C*). *Cygb*-cDNA-ADV significantly increased the percentage of time spent in the quadrant as compared with the HI group ($p < 0.01$; Fig. 8*C*). These results demonstrated a long term neuroprotective effect of CYGB on HI brain injury.

DISCUSSION

Perinatal HI brain injury is a major cause of morbidity and mortality in infants and children (1, 2), and an increasing number of studies are being conducted to investigate the pathogenesis of the disease. In the present study, we show for the first time that CYGB is neuroprotective in neonatal rats exposed to HI through possible antioxidative and antiapoptotic mechanisms and by promoting angiogenesis (Fig. 9). First, we identified the endogenous up-regulation patterns of *Cygb* mRNA and protein in the developing brain under the condition of HI brain injury. Moreover, we found that changes in *Cygb* expression result in corresponding changes in the severity of histological and functional deficits after HI, in a manner consistent with an endogenous neuroprotective action of CYGB. In summary, this study suggests that CYGB plays an important role in the signaling pathway underlying oxidative stress, angiogenesis, and neuronal apoptosis in the neonatal HI rat model.

Although several previous studies have demonstrated that *Cygb* is affected by hypoxia *in vitro* (16, 21, 42) and *in vivo* (17, 18, 20, 42, 43), the detailed expression patterns *of Cygb* mRNA and protein in neonatal rats brain suffering from HI have not been reported until now. The present study is the first to undertake a comprehensive analysis of CYGB expression in response to neonatal rat brain HI injury at the acute stage. Our study demonstrates that CYGB is significantly up-regulated at both transcriptional and translational levels in a time-dependent manner. However, it must be noted that two previous studies reported that the expression of CYGB was not significantly up-regulated in the ischemic model of adult rats (44, 45). A possible explanation for the paradoxical findings is that there were some limitations in these two studies, such that no detailed data were presented to illustrate the changes in CYGB expression during the first 36 h after ischemia, and different animal models that only suffered ischemic treatment were used. Moreover, it is possible that the age of the rats also contributed to the differences in results. Because we found that the expression of CYGB protein peaks at 24 h post-HI (Fig. 2), it appears that CYGB is up-regulated during the acute stage of HI. Based on previous data for CYGB expression change under hypoxic conditions *in vivo* and *in vitro* (18, 19, 42, 43), another possible explanation for the discrepancy is that hypoxia may play a more important role than ischemia in up-regulating *Cygb* expression. Because there were significantly higher *Cygb* mRNA and protein levels in neonatal HI injury rats compared with sham rats, which points to an important role of *Cygb* in hypoxia-ischemia adaptation, RNA-interfering technology was used, and a *Cygb* knockdown model was successfully established using the *Cygb*-shRNA-ADV system 4 days before HI induction (Fig. 3). Significantly aggravated brain injuries were observed at 24 h after HI (Fig. 5). Cognitive functions were also impaired severely under conditions of HI in the *Cygb*-shRNA-ADV group, as demonstrated by the performance of the MWM test (Fig. 8). These data indicated that CYGB is a novel endogenous neuroprotective factor in the neonatal HI model.

Many investigators have explored the development of therapeutic methods for neonatal HI disease. Although hypothermia, the most widely applied clinical intervention in asphyxiated babies, improves outcome, the efficiency is limited because it is only mildly effective for children born at term (46, 47). Our study focused on the effect of *Cygb* overexpression in HI injury and was initially stimulated by the application of gene therapy to various brain diseases. The results showed that *Cygb* overexpression attenuated cerebral infarction and neuron cell apoptosis caused by HI in the neonatal brain (Fig. 5). The protective effect improved long term neurological function 3 weeks after HI insult (Fig. 8); thus, we propose that CYGB functions as an endogenous neuroprotective protein, providing a new therapeutic target for neonatal HI disease.

Previous findings have shown that CYGB is expressed in distinct regions of the mouse brain as compared with neuroglobin, and these regions (hippocampus, thalamus, and hypothalamus) play an important role in protecting from oxidative stress (20). As compared with the adult brain, the immature brain is highly susceptible to oxidative stress because of its high concentration of unsaturated fatty acids, rate of oxygen consumption, and availability of redox-active iron but poorly developed scavenging systems (48). Therefore, oxidative stress is thought to be

FIGURE 5. *A*, assessment of infarct volume in neonatal brain induced by HI using TTC staining. Data from both TTC staining and Nissl staining showed that overexpression of CYGB reduced brain tissue loss (*B* and *E*). *C*, representative photomicrographs of Nissl staining for observing the morphology of neurons in the cortex and hippocampus (CA1) of neonatal rat brains from different groups shown at two different magnifications (*scale bars*, 20 μm (*main panel*) and 200 μm (*inset*)). In the sham group of Nissl staining, the neuronal cell outline was clear, and the structure was compact with abundant cytoplasm and cell body; however, evident neuronal loss and neuronal degeneration were observed in the HI group, saline, ADV vector, and shRNA groups with cells arranged sparsely with vague cell outlines. The number of cells with eumorphism was significantly reduced. Injection of *Cygb*-cDNA-ADV substantially increased the proportion of neurons that survived. TUNEL staining showed apoptosis in the cortex and hippocampus (CA1) of neonatal rat brains from different groups (*D*). *Scale bar*, 200 μm. The number of positive cells (*dark brown*, *arrows* indicate TUNEL-positive cells) was much lower in *Cygb*-cDNA-ADV brains than in HI brains (*F*). *Diagonal arrows*, TUNEL-positive cells. *E* and *F*, cell counts/visual field ($\times$ 400) found in the slides with Nissl staining and TUNEL staining. The data are expressed as mean $\pm$ S.D. (*error bars*) ($n = 8$). *a*, $p < 0.01$ as compared with the sham group; *b*, no significant difference; *c*, $p < 0.01$ as compared with the HI group.

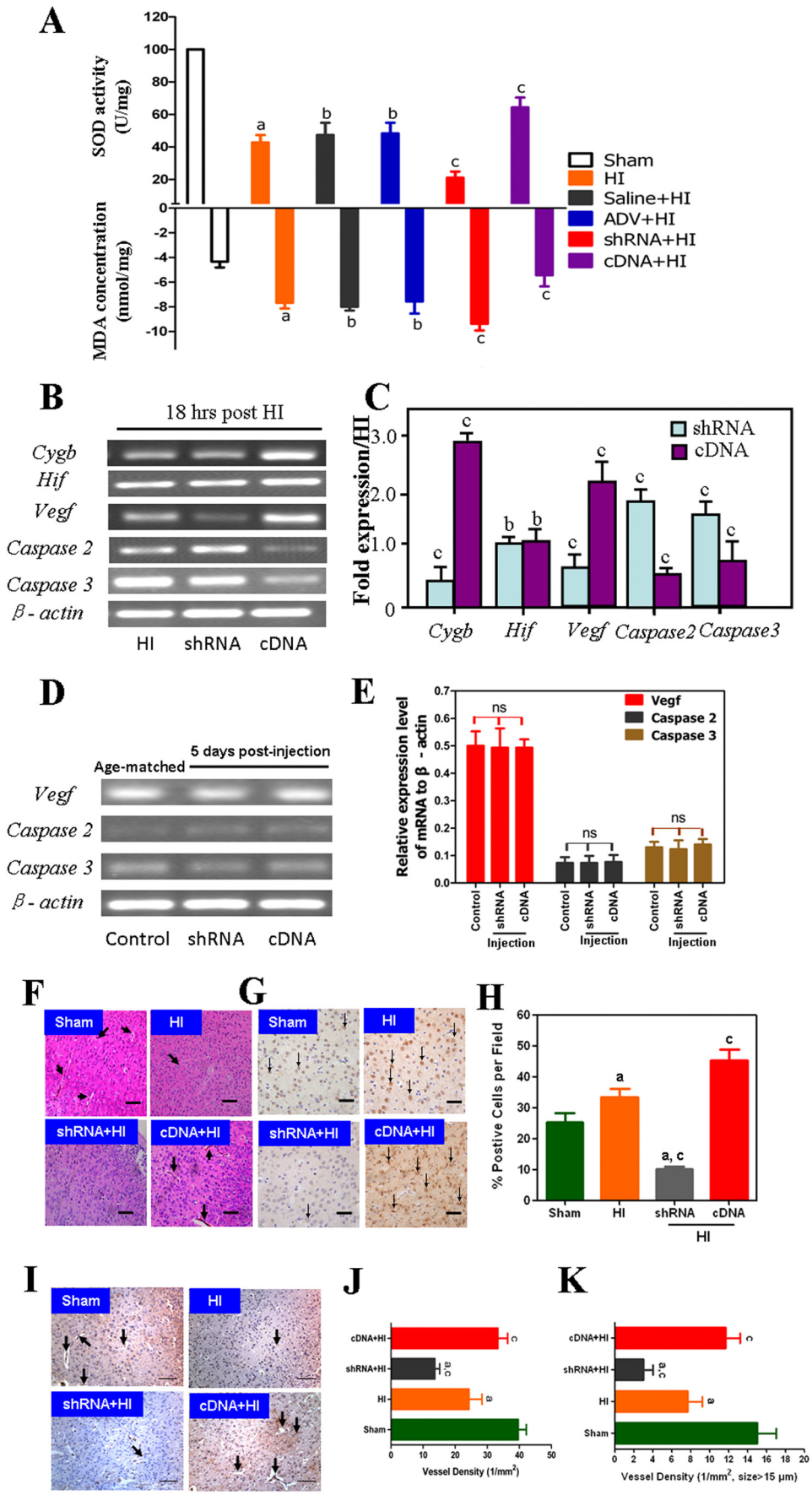
A
SOD activity (U/mg)
MDA concentration (nmol/mg)
Sham
HI
Saline+HI
ADV+HI
shRNA+HI
cDNA+HI
B
18 hrs post HI
Cygb
Hif
Vegf
Caspase 2
Caspase 3
β - actin
HI
shRNA
cDNA
C
Fold expression/HI
shRNA
cDNA
Cygb
Hif
Vegf
Caspase2
Caspase3
D
Age-matched
5 days post-injection
Vegf
Caspase 2
Caspase 3
β - actin
Control
shRNA
cDNA
E
Relative expression level of mRNA to β - actin
Vegf
Caspase 2
Caspase 3
ns
Control
shRNA
cDNA
Injection
F
G
Sham
HI
shRNA+HI
cDNA+HI
H
% Postive Cells per Field
Sham
HI
shRNA
cDNA
I
Sham
HI
shRNA+HI
cDNA+HI
J
Vessel Density (1/mm²)
K
Vessel Density (1/mm², size>15 μm)

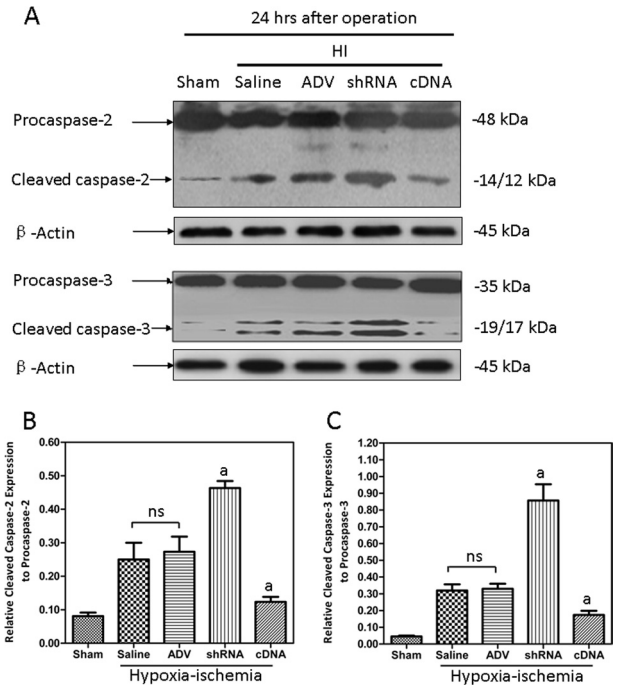

FIGURE 7. **The activation of both caspase-2 and caspase-3 induced by HI were suppressed by CYGB overexpression.** *A*, representative electrophoretic images for both the activation of caspase-2 (*top*) and caspase-3 (*bottom*) from different groups. The results showed that the active levels of caspase-2 and caspase-3 protein were suppressed by CYGB (*B* and *C*). Results are presented as mean ± S.D. (*error bars*) in triplicate independent experiments ($n = 3$). *a*, $p < 0.01$ as compared with HI group; *ns*, not significant.

one of the major factors that induce neuronal cell death in the immature brain (49). In this study, MDA and SOD activity were measured to confirm the antioxidant role of CYGB *in vivo*. The results indicated that CYGB could increase neonatal tolerance to HI partly due to its antioxidative effect at the early stage of HI injury. The antioxidant effects of CYGB have recently been investigated, and emerging evidence has demonstrated a protective role of CYGB against oxidative stress, especially in models of fibrosis that involve hypoxic reperfusion and subsequent oxidative injury (19, 25, 50–53). It was also reported that CYGB expression protected neuronal cells from oxidative damage *in vitro* (21, 22, 54, 55); however, it is unclear whether this is a direct antioxidative effect of CYGB under HI conditions. Downstream signaling in the CYGB pathway may result in these antioxidative effects. Due to its NO dioxygenase activity (56–58), CYGB might reduce intracellular NO concentration, which in turn may prevent accumulation of peroxynitrite, a strong oxidant formed from the reaction between superoxide and NO. It has been speculated that CYGB, like other hexacoordinated globins, may eliminate reactive oxygen species utilizing heme and thiol residues (59, 60), and it has been found that CYGB may reduce the induction of intracellular reactive oxygen species formation (55, 61). The processes of lipid-induced transformation of CYGB from hexacoordinate to pentacoordinate may allow the cell to up-regulate antioxidant defenses before extensive oxidative damage occurs (62). Nevertheless, additional studies are required to confirm the pathways and mechanisms of the protein in protecting brain HI damage from oxidative stress.

In our study, we show that CYGB mediates a neuroprotective effect through reducing cerebral infractions and apoptosis caused by oxidative stress *in vivo*. Furthermore, the molecular mechanisms and signal pathways that are responsible for the neuroprotective property of CYGB are also of great interest. Fordel *et al.* reported that the up-regulation of *Cygb*, as well as the *Vegf* gene, was abrogated in brain tissue of *Hif-1* knock-out mice upon hypoxia (42, 63) and found that the mechanism of *Cygb* induction is *Hif-1α*-dependent (63). Guo *et al.* (64) proposed that *Hif-1* could regulate CYGB expression by binding to hypoxia-responsive elements of the protein, which was confirmed in 2009 by Singh *et al.* (19). Our results show that *Hif-1α* was not affected by *Cygb*, supporting the assumption that *Hif-1α* might be the upstream gene of *Cygb in vivo* under HI conditions. In present study, we found that ischemic infarction could be affected by different expression levels of CYGB (Fig. 5, *A* and *B*), and both the *Vegf* mRNA and protein expression levels were regulated by CYGB (Fig. 6), which is consistent with previous findings that CYGB may induce the induction and synthesis of *Vegf in vitro* (16). We also show that *Cygb* overexpression increased both the density and diameter of microvessels in brain tissue under HI conditions, due at least in part to the *Vegf* up-regulation. *Vegf* was found to increase phosphorylation of protein kinase B (Akt) and extracellular-signal regulated kinase 1/2 (ERK1/2) in the cortex in the neonatal rat HI model (65). Jones and Bergeron (66) have found that activation of ERK1/2 contributes to HI tolerance in the neonatal brain in part by preserving vascular and white matter integrity. A role for ERK1/2 in neurons has been demonstrated in neuronal gene expression regulation (CREB, Elk-1, and c-Myc) and long term potentiation and memory formation (67). Dash and co-workers (68, 69) demonstrated ERK activation in the hippocampus and cortex during MWM training, which is consistent with our results that CYGB can promote long term spatial learning and memory abilities. These findings are strengthened by data suggesting that *Vegf* can reduce infarct size, improve neurological performance, markedly enhance angiogenesis in the ischemic brain, and reduce neurological deficits during stroke recovery (39, 70). Thus, we believe that the *"Hif-1α-Cygb-Vegf"* signaling

FIGURE 6. ***Cygb* exerts its neuroprotective activity via antioxidant and antiapoptotic mechanisms but also promotes angiogenesis.** *A*, the comparison of MDA level and SOD activity among different groups ($n = 8$). SOD activity was higher in the cDNA treatment group but lower in the shRNA group as compared with the HI group. *B*, representative image of *Cygb*-related genes. RT-PCR showed that overexpression of *Cygb* leads to up-regulation of the transcriptional level of *Vegf*, which plays a crucial role in promoting angiogenesis but down-regulates apoptosis-related genes, caspase-2 and -3 (*C*). β-Actin was used as an internal control. The expression of *Vegf*, caspase-2, and caspase-3 was not affected by *Cygb* transfection under normal conditions (*D* and *E*). The data are expressed as mean ± S.D. (*error bars*) in triplicate independent experiments ($n = 3$). Disrupted microvessels and cell morphology in both HE and anti-CD31 staining images of the ischemic border areas from sham, HI, shRNA + HI, and cDNA + HI groups are shown. *Arrowhead*, microvessels; *scale bar*, 200 μm (*F* and *I*). Representative images of VEGF immunostaining from the corresponding groups show that the expression of VEGF protein is CYGB-dependent under HI conditions. ↓, VEGF-positive cells (*G*). A quantification of VEGF-positive cells/field is also shown (*H*). *J* and *K*, immunohistochemical staining of CD31 and the number and diameter of microvessels in different groups are expressed as mean ± S.D. in triplicate independent experiments ($n = 3$). *a*, $p < 0.01$ as compared with the sham group. *b* and *ns*, no significant difference; *c*, $p < 0.01$ as compared with the HI group.

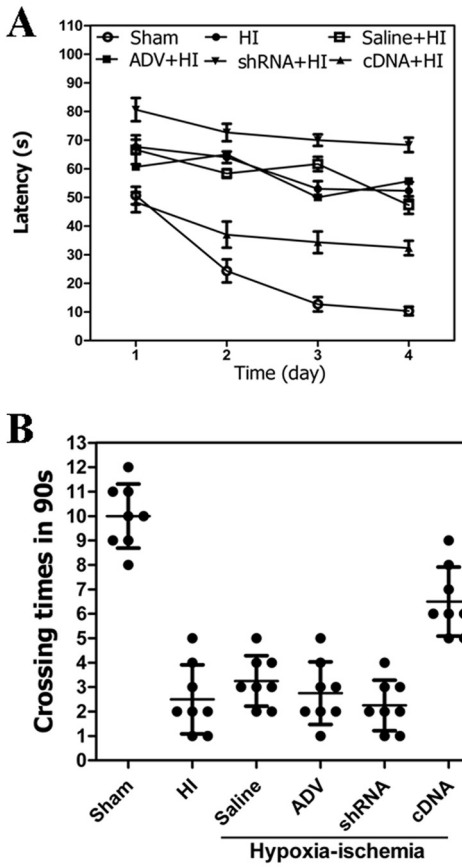

FIGURE 8. **Results from the Morris water maze tests ($n = 8$).** Repeated measures analysis of variance revealed statistically significant differences ($p < 0.01$) (day/group interaction) between the HI, shRNA, and cDNA groups but did not reveal differences between the saline or ADV-null vector injection groups (*A*). ▼, *Cygb*-shRNA-ADV injection + HI group; ●, HI group; □, saline injection + HI group; ■, ADV vectors only + HI group; ▲, *Cygb*-cDNA-ADV injection + HI group; ○, sham group. On the first day, the EL values of these groups were narrow in range. On the fourth day, the EL values of the shRNA group were higher as compared with the HI group; however, EL values in the *Cygb*-cDNA injection group were much lower than those in the HI group ($p < 0.01$). On the fifth day, the sham group had a short swim path to the former platform location, whereas the rats of the other groups had longer swim paths. The platform crossing (swimming into the area where the former platform was located within 90 s after removing the platform) was lower in the HI, saline, and ADV only groups compared with the sham group ($p < 0.01$). *B*, the number of platform crossings in the shRNA injection group was lower compared with the HI model group ($p < 0.05$) and also significantly less compared with the cDNA injection group ($p < 0.01$). *C*, comparison of the percentage of time spent in the target quadrant among different groups. *a*, $p < 0.01$ as compared with the sham group. *b*, significant difference; *c*, $p < 0.01$ as compared with the HI group. *Error bars*, S.D.

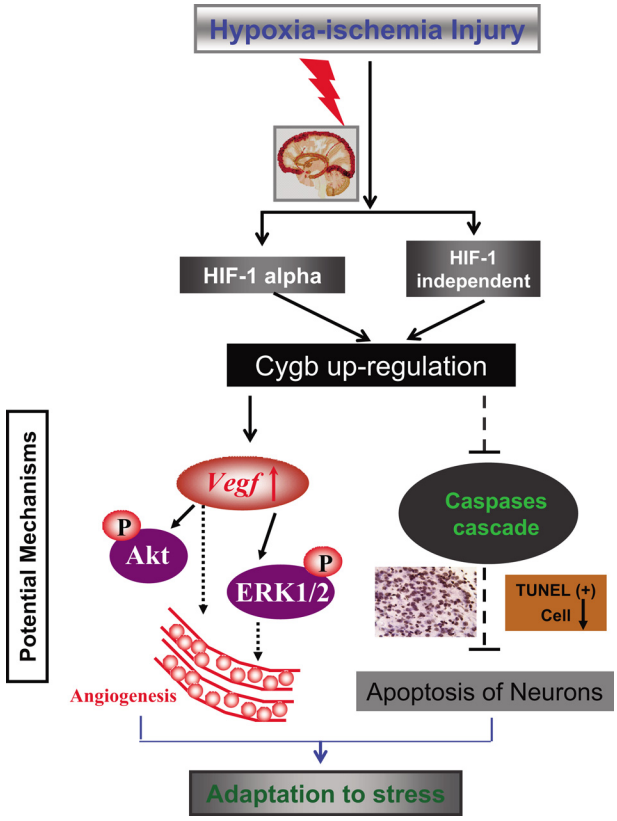

FIGURE 9. **Schematic of possible mechanisms by which *Cygb* reduces brain tissue loss and improves long term learning and memory abilities under conditions of neonatal HI.** *Hif-1α* was induced by hypoxia-ischemia, and *Cygb* expression was enhanced by *Hif-1α*. Expression of *Vegf*, which could promote angiogenesis, may be up-regulated by *Cygb* overexpression. *Cygb* may exert its antiapoptotic function via negative regulation of caspase-2 and -3 expression, potentially leading to reversal of impairments in neonatal rats that suffered from HI.

pathway might be an important part in the CYGB antioxidant mechanism to protect neurons against HI injury in neonatal brain and reduce infarct. An *in vitro* model confirming this *"Hif-1α-Cygb-Vegf"* signaling pathway is needed for future study. In addition, it remains to be tested whether other signal molecules may also act as upstream mediators of CYGB *in vivo*, such as erythropoietin, which has been confirmed to have antioxidative effects by regulating several downstream genes, including *Cygb* (64).

Because previous studies of CYGB mainly focused on nitric-oxide dioxygenase and lipid peroxidase activities, the role of CYGB in the process of cell apoptosis remains unknown. Apoptosis is one of many key factors contributing to the injury of developmental brain induced by HI or other insults. Caspase inhibitors have been reported to provide neuroprotection in neonatal rat models (71). Caspase-2 is a developmentally regulated initiator caspase, and recent data have demonstrated that caspase-2 mediates HI brain injury (38). In our study, results from a TUNEL apoptosis assay indicated that the number of apoptotic cells decreased in both the cortex and hippocampus after the neonatal *Cygb* overexpression rats were subjected to HI. Our findings demonstrate that *Cygb* overexpression suppresses the activation of caspase-2 and -3. These findings indicate that the caspase family members are downstream targets in the antiapoptotic effects of CYGB. In the present study, we show that the antiapoptotic function of CYGB in the neonatal brain was achieved in part through the negative regulation of expression of caspase-2 and -3. Previous studies have reported

that genetic inhibition of caspase-2 could reduce neonatal HI brain injury and that caspase-3 activity was also attenuated by inhibition of caspase-2, indicating that caspase-3 is the downstream gene of caspase-2 (38). Caspase-3 has also been demonstrated to own a role in regulating ischemic neuronal injury (72), mediated by *Vegf*, in the regulation of neuronal death under hypoxia (73). Several studies have also suggested that caspase-2 induced mitochondrial outer membrane permeabilization, which led to the release of proapoptotic molecules from mitochondria, such as the release of cytochrome *c* (74–76) by direct processing of full-length Bid to activated truncated tBid (77). Interestingly, ERK was reported to protect hypoxic cortical neurons via phosphorylation of Bid (78). Thus, it is possible that CYGB plays a neuroprotective role against HI injury partially due to reduction of oxidative stress-mediated caspase-dependent apoptosis.

In conclusion, CYGB is up-regulated by HI in the neonatal brain. Using a gene transfection technique, we demonstrated for the first time that CYGB displayed significant functions of neuronal protection and repair in the HI-injured neonatal brain. Also, for the first time, it is proposed that CYGB might exert its protective activity by molecular mechanisms of antioxidant and antiapoptosis and that the effects of reducing infarct might occur through regulating VEGF and CD31 expression, thus affecting angiogenesis. Nevertheless, further investigation is required to explain the mechanism by which CYGB contributes to the molecular pathogenesis of neonatal brain HI disease and to pursue the utilization of CYGB in the clinical management of such disorders.

Acknowledgments—The experiments were mainly carried out in the Laboratory of Research Center for Reproductive Medicine, Shantou University Medical College. We acknowledge the invaluable help of Jian-Kun Xu (Prince of Wales Hospital, Chinese University of Hong Kong, Shatin, New Territories, Hong Kong).

REFERENCES

1. du Plessis, A. J., and Volpe, J. J. (2002) Perinatal brain injury in the preterm and term newborn. *Curr. Opin. Neurol.* **15,** 151–157
2. Ferriero, D. M. (2004) Neonatal brain injury. *N. Engl. J. Med.* **351,** 1985–1995
3. Bass, J. L., Corwin, M., Gozal, D., Moore, C., Nishida, H., Parker, S., Schonwald, A., Wilker, R. E., Stehle, S., and Kinane, T. B. (2004) The effect of chronic or intermittent hypoxia on cognition in childhood. A review of the evidence. *Pediatrics* **114,** 805–816
4. Nelson, K. B., and Lynch, J. K. (2004) Stroke in newborn infants. *Lancet Neurol.* **3,** 150–158
5. Trent, J. T., 3rd, and Hargrove, M. S. (2002) A ubiquitously expressed human hexacoordinate hemoglobin. *J. Biol. Chem.* **277,** 19538–19545
6. Burmester, T., Weich, B., Reinhardt, S., and Hankeln, T. (2000) A vertebrate globin expressed in the brain. *Nature* **407,** 520–523
7. Sun, Y., Jin, K., Mao, X. O., Zhu, Y., and Greenberg, D. A. (2001) Neuroglobin is up-regulated by and protects neurons from hypoxic-ischemic injury. *Proc. Natl. Acad. Sci. U.S.A.* **98,** 15306–15311
8. Venis, S. (2001) Neuroglobin might protect brain cells during stroke. *Lancet* **358,** 2055
9. Sun, Y., Jin, K., Peel, A., Mao, X. O., Xie, L., and Greenberg, D. A. (2003) Neuroglobin protects the brain from experimental stroke *in vivo*. *Proc. Natl. Acad. Sci. U.S.A.* **100,** 3497–3500
10. Jin, K., Mao, Y., Mao, X., Xie, L., and Greenberg, D. A. (2010) Neuroglobin expression in ischemic stroke. *Stroke* **41,** 557–559
11. Yu, Z., Liu, N., Liu, J., Yang, K., and Wang, X. (2012) Neuroglobin, a novel target for endogenous neuroprotection against stroke and neurodegenerative disorders. *Int. J. Mol. Sci.* **13,** 6995–7014
12. Hoogewijs, D., Ebner, B., Germani, F., Hoffmann, F. G., Fabrizius, A., Moens, L., Burmester, T., Dewilde, S., Storz, J. F., Vinogradov, S. N., and Hankeln, T. (2012) Androglobin. A chimeric globin in metazoans that is preferentially expressed in mammalian testes. *Mol. Biol. Evol.* **29,** 1105–1114
13. Burmester, T., Ebner, B., Weich, B., and Hankeln, T. (2002) Cytoglobin. A novel globin type ubiquitously expressed in vertebrate tissues. *Mol. Biol. Evol.* **19,** 416–421
14. Pesce, A., Bolognesi, M., Bocedi, A., Ascenzi, P., Dewilde, S., Moens, L., Hankeln, T., and Burmester, T. (2002) Neuroglobin and cytoglobin. Fresh blood for the vertebrate globin family. *EMBO Rep.* **3,** 1146–1151
15. Geuens, E., Brouns, I., Flamez, D., Dewilde, S., Timmermans, J. P., and Moens, L. (2003) A globin in the nucleus! *J. Biol. Chem.* **278,** 30417–30420
16. Stagner, J. I., Parthasarathy, S. N., Wyler, K., and Parthasarathy, R. N. (2005) Protection from ischemic cell death by the induction of cytoglobin. *Transplant. Proc.* **37,** 3452–3453
17. Hankeln, T., Ebner, B., Fuchs, C., Gerlach, F., Haberkamp, M., Laufs, T. L., Roesner, A., Schmidt, M., Weich, B., Wystub, S., Saaler-Reinhardt, S., Reuss, S., Bolognesi, M., De Sanctis, D., Marden, M. C., Kiger, L., Moens, L., Dewilde, S., Nevo, E., Avivi, A., Weber, R. E., Fago, A., and Burmester, T. (2005) Neuroglobin and cytoglobin in search of their role in the vertebrate globin family. *J. Inorg. Biochem.* **99,** 110–119
18. Avivi, A., Gerlach, F., Joel, A., Reuss, S., Burmester, T., Nevo, E., and Hankeln, T. (2010) Neuroglobin, cytoglobin, and myoglobin contribute to hypoxia adaptation of the subterranean mole rat Spalax. *Proc. Natl. Acad. Sci. U.S.A.* **107,** 21570–21575
19. Singh, S., Manda, S. M., Sikder, D., Birrer, M. J., Rothermel, B. A., Garry, D. J., and Mammen, P. P. (2009) Calcineurin activates cytoglobin transcription in hypoxic myocytes. *J. Biol. Chem.* **284,** 10409–10421
20. Mammen, P. P., Shelton, J. M., Ye, Q., Kanatous, S. B., McGrath, A. J., Richardson, J. A., and Garry, D. J. (2006) Cytoglobin is a stress-responsive hemoprotein expressed in the developing and adult brain. *J. Histochem. Cytochem.* **54,** 1349–1361
21. Li, D., Chen, X. Q., Li, W. J., Yang, Y. H., Wang, J. Z., and Yu, A. C. (2007) Cytoglobin up-regulated by hydrogen peroxide plays a protective role in oxidative stress. *Neurochem. Res.* **32,** 1375–1380
22. Fang, J., Ma, I., and Allalunis-Turner, J. (2011) Knockdown of cytoglobin expression sensitizes human glioma cells to radiation and oxidative stress. *Radiat. Res.* **176,** 198–207
23. Shivapurkar, N., Stastny, V., Okumura, N., Girard, L., Xie, Y., Prinsen, C., Thunnissen, F. B., Wistuba, I. I., Czerniak, B., Frenkel, E., Roth, J. A., Liloglou, T., Xinarianos, G., Field, J. K., Minna, J. D., and Gazdar, A. F. (2008) Cytoglobin, the newest member of the globin family, functions as a tumor suppressor gene. *Cancer Res.* **68,** 7448–7456
24. Xinarianos, G., McRonald, F. E., Risk, J. M., Bowers, N. L., Nikolaidis, G., Field, J. K., and Liloglou, T. (2006) Frequent genetic and epigenetic abnormalities contribute to the deregulation of cytoglobin in non-small cell lung cancer. *Hum. Mol. Genet.* **15,** 2038–2044
25. Nishi, H., Inagi, R., Kawada, N., Yoshizato, K., Mimura, I., Fujita, T., and Nangaku, M. (2011) Cytoglobin, a novel member of the globin family, protects kidney fibroblasts against oxidative stress under ischemic conditions. *Am. J. Pathol.* **178,** 128–139
26. Klaunig, J. E., and Kamendulis, L. M. (2004) The role of oxidative stress in carcinogenesis. *Annu. Rev. Pharmacol. Toxicol.* **44,** 239–267
27. Valko, M., Izakovic, M., Mazur, M., Rhodes, C. J., and Telser, J. (2004) Role of oxygen radicals in DNA damage and cancer incidence. *Mol. Cell Biochem.* **266,** 37–56
28. Rice, J. E., 3rd, Vannucci, R. C., and Brierley, J. B. (1981) The influence of immaturity on hypoxic-ischemic brain damage in the rat. *Ann. Neurol.* **9,** 131–141
29. Sugiura, S., Kitagawa, K., Tanaka, S., Todo, K., Omura-Matsuoka, E., Sasaki, T., Mabuchi, T., Matsushita, K., Yagita, Y., and Hori, M. (2005) Adenovirus-mediated gene transfer of heparin-binding epidermal growth factor-like growth factor enhances neurogenesis and angiogenesis after

focal cerebral ischemia in rats. *Stroke* **36,** 859–864
30. Shinozaki, K., Ebert, O., Suriawinata, A., Thung, S. N., and Woo, S. L. (2005) Prophylactic α interferon treatment increases the therapeutic index of oncolytic vesicular stomatitis virus virotherapy for advanced hepatocellular carcinoma in immune-competent rats. *J. Virol.* **79,** 13705–13713
31. Sagawa, T., Yamada, Y., Takahashi, M., Sato, Y., Kobune, M., Takimoto, R., Fukaura, J., Iyama, S., Sato, T., Miyanishi, K., Matsunaga, T., Takayama, T., Kato, J., Sasaki, K., Hamada, H., and Niitsu, Y. (2008) Treatment of hepatocellular carcinoma by AdAFPep/rep, AdAFPep/p53, and 5-fluorouracil in mice. *Hepatology* **48,** 828–840
32. Zheng, F. Q., Xu, Y., Yang, R. J., Wu, B., Tan, X. H., Qin, Y. D., and Zhang, Q. W. (2009) Combination effect of oncolytic adenovirus therapy and herpes simplex virus thymidine kinase/ganciclovir in hepatic carcinoma animal models. *Acta Pharmacol. Sin.* **30,** 617–627
33. Chen, W., Ma, Q., Suzuki, H., Hartman, R., Tang, J., and Zhang, J. H. (2011) Osteopontin reduced hypoxia-ischemia neonatal brain injury by suppression of apoptosis in a rat pup model. *Stroke* **42,** 764–769
34. Xu, J. K., Chen, H. J., Li, X. D., Huang, Z. L., Xu, H., Yang, H. L., and Hu, J. (2012) Optimal intensity shock wave promotes the adhesion and migration of rat osteoblasts via integrin β1-mediated expression of phosphorylated focal adhesion kinase. *J. Biol. Chem.* **287,** 26200–26212
35. Liu, F., Schafer, D. P., and McCullough, L. D. (2009) TTC, fluoro-Jade B, and NeuN staining confirm evolving phases of infarction induced by middle cerebral artery occlusion. *J. Neurosci. Methods* **179,** 1–8
36. Huang, Y., Shi, X., Xu, H., Yang, H., Chen, T., Chen, S., and Chen, X. (2010) Chronic unpredictable stress before pregnancy reduce the expression of brain-derived neurotrophic factor and *N*-methyl-D-aspartate receptor in hippocampus of offspring rats associated with impairment of memory. *Neurochem. Res.* **35,** 1038–1049
37. Semenza, G. L. (2001) HIF-1 and mechanisms of hypoxia sensing. *Curr. Opin. Cell Biol.* **13,** 167–171
38. Carlsson, Y., Schwendimann, L., Vontell, R., Rousset, C. I., Wang, X., Lebon, S., Charriaut-Marlangue, C., Supramaniam, V., Hagberg, H., Gressens, P., and Jacotot, E. (2011) Genetic inhibition of caspase-2 reduces hypoxic-ischemic and excitotoxic neonatal brain injury. *Ann. Neurol.* **70,** 781–789
39. Sun, Y., Jin, K., Xie, L., Childs, J., Mao, X. O., Logvinova, A., and Greenberg, D. A. (2003) VEGF-induced neuroprotection, neurogenesis, and angiogenesis after focal cerebral ischemia. *J. Clin. Invest.* **111,** 1843–1851
40. Greenberg, D. A., Jin, K., and Khan, A. A. (2008) Neuroglobin. An endogenous neuroprotectant. *Curr. Opin. Pharmacol.* **8,** 20–24
41. D'Hooge, R., and De Deyn, P. P. (2001) Applications of the Morris water maze in the study of learning and memory. *Brain Res. Brain Res. Rev.* **36,** 60–90
42. Fordel, E., Geuens, E., Dewilde, S., Rottiers, P., Carmeliet, P., Grooten, J., and Moens, L. (2004) Cytoglobin expression is upregulated in all tissues upon hypoxia. An *in vitro* and *in vivo* study by quantitative real-time PCR. *Biochem. Biophys. Res. Commun.* **319,** 342–348
43. Schmidt, M., Gerlach, F., Avivi, A., Laufs, T., Wystub, S., Simpson, J. C., Nevo, E., Saaler-Reinhardt, S., Reuss, S., Hankeln, T., and Burmester, T. (2004) Cytoglobin is a respiratory protein in connective tissue and neurons, which is up-regulated by hypoxia. *J. Biol. Chem.* **279,** 8063–8069
44. Büttner, F., Cordes, C., Gerlach, F., Heimann, A., Alessandri, B., Luxemburger, U., Türeci, O., Hankeln, T., Kempski, O., and Burmester, T. (2009) Genomic response of the rat brain to global ischemia and reperfusion. *Brain Res.* **1252,** 1–14
45. Raida, Z., Reimets, R., Hay-Schmidt, A., and Hundahl, C. A. (2012) Effect of permanent middle cerebral artery occlusion on Cytoglobin expression in the mouse brain. *Biochem. Biophys. Res. Commun.* **424,** 274–278
46. Gluckman, P. D., Wyatt, J. S., Azzopardi, D., Ballard, R., Edwards, A. D., Ferriero, D. M., Polin, R. A., Robertson, C. M., Thoresen, M., Whitelaw, A., and Gunn, A. J. (2005) Selective head cooling with mild systemic hypothermia after neonatal encephalopathy. Multicentre randomised trial. *Lancet* **365,** 663–670
47. Azzopardi, D. V., Strohm, B., Edwards, A. D., Dyet, L., Halliday, H. L., Juszczak, E., Kapellou, O., Levene, M., Marlow, N., Porter, E., Thoresen, M., Whitelaw, A., and Brocklehurst, P. (2009) Moderate hypothermia to treat perinatal asphyxial encephalopathy. *N. Engl. J. Med.* **361,** 1349–1358
48. Ferriero, D. M. (2001) Oxidant mechanisms in neonatal hypoxia-ischemia. *Dev. Neurosci.* **23,** 198–202
49. Greggio, S., de Paula, S., de Oliveira, I. M., Trindade, C., Rosa, R. M., Henriques, J. A., and DaCosta, J. C. (2011) NAP prevents acute cerebral oxidative stress and protects against long-term brain injury and cognitive impairment in a model of neonatal hypoxia-ischemia. *Neurobiol. Dis.* **44,** 152–159
50. Xu, R., Harrison, P. M., Chen, M., Li, L., Tsui, T. Y., Fung, P. C., Cheung, P. T., Wang, G., Li, H., Diao, Y., Krissansen, G. W., Xu, S., and Farzaneh, F. (2006) Cytoglobin overexpression protects against damage-induced fibrosis. *Mol. Ther.* **13,** 1093–1100
51. Kawada, N., Kristensen, D. B., Asahina, K., Nakatani, K., Minamiyama, Y., Seki, S., and Yoshizato, K. (2001) Characterization of a stellate cell activation-associated protein (STAP) with peroxidase activity found in rat hepatic stellate cells. *J. Biol. Chem.* **276,** 25318–25323
52. Stagner, J. I., Seelan, R. S., Parthasarathy, R. N., and White, K. (2009) Reduction of ischemic cell death in cultured islets of Langerhans by the induction of cytoglobin. *Islets* **1,** 50–54
53. Mimura, I., Nangaku, M., Nishi, H., Inagi, R., Tanaka, T., and Fujita, T. (2010) Cytoglobin, a novel globin, plays an antifibrotic role in the kidney. *Am. J. Physiol. Renal Physiol.* **299,** F1120–F1133
54. Fordel, E., Thijs, L., Martinet, W., Lenjou, M., Laufs, T., Van Bockstaele, D., Moens, L., and Dewilde, S. (2006) Neuroglobin and cytoglobin overexpression protects human SH-SY5Y neuroblastoma cells against oxidative stress-induced cell death. *Neurosci. Lett.* **410,** 146–151
55. Hodges, N. J., Innocent, N., Dhanda, S., and Graham, M. (2008) Cellular protection from oxidative DNA damage by over-expression of the novel globin cytoglobin *in vitro*. *Mutagenesis* **23,** 293–298
56. Gardner, A. M., Cook, M. R., and Gardner, P. R. (2010) Nitric-oxide dioxygenase function of human cytoglobin with cellular reductants and in rat hepatocytes. *J. Biol. Chem.* **285,** 23850–23857
57. Halligan, K. E., Jourd'heuil, F. L., and Jourd'heuil, D. (2009) Cytoglobin is expressed in the vasculature and regulates cell respiration and proliferation via nitric oxide dioxygenation. *J. Biol. Chem.* **284,** 8539–8547
58. Li, H., Hemann, C., Abdelghany, T. M., El-Mahdy, M. A., and Zweier, J. L. (2012) Characterization of the mechanism and magnitude of cytoglobin-mediated nitrite reduction and nitric oxide generation under anaerobic conditions. *J. Biol. Chem.* **287,** 36623–36633
59. Petersen, M. G., Dewilde, S., and Fago, A. (2008) Reactions of ferrous neuroglobin and cytoglobin with nitrite under anaerobic conditions. *J. Inorg. Biochem.* **102,** 1777–1782
60. Fordel, E., Thijs, L., Martinet, W., Schrijvers, D., Moens, L., and Dewilde, S. (2007) Anoxia or oxygen and glucose deprivation in SH-SY5Y cells. A step closer to the unraveling of neuroglobin and cytoglobin functions. *Gene* **398,** 114–122
61. De Beuf, A., Hou, X. H., D'Haese, P. C., and Verhulst, A. (2010) Epoetin δ reduces oxidative stress in primary human renal tubular cells. *J. Biomed. Biotechnol.* **2010,** 395785
62. Reeder, B. J., Svistunenko, D. A., and Wilson, M. T. (2011) Lipid binding to cytoglobin leads to a change in haem co-ordination. A role for cytoglobin in lipid signalling of oxidative stress. *Biochem. J.* **434,** 483–492
63. Fordel, E., Geuens, E., Dewilde, S., De Coen, W., and Moens, L. (2004) Hypoxia/ischemia and the regulation of neuroglobin and cytoglobin expression. *IUBMB Life* **56,** 681–687
64. Guo, X., Philipsen, S., and Tan-Un, K. C. (2007) Study of the hypoxia-dependent regulation of human CYGB gene. *Biochem. Biophys. Res. Commun.* **364,** 145–150
65. Feng, Y., Rhodes, P. G., and Bhatt, A. J. (2008) Neuroprotective effects of vascular endothelial growth factor following hypoxic ischemic brain injury in neonatal rats. *Pediatr. Res.* **64,** 370–374
66. Jones, N. M., and Bergeron, M. (2004) Hypoxia-induced ischemic tolerance in neonatal rat brain involves enhanced ERK1/2 signaling. *J. Neurochem.* **89,** 157–167
67. Sweatt, J. D. (2001) The neuronal MAP kinase cascade. A biochemical signal integration system subserving synaptic plasticity and memory. *J. Neurochem.* **76,** 1–10
68. Blum, S., Moore, A. N., Adams, F., and Dash, P. K. (1999) A mitogen-

activated protein kinase cascade in the CA1/CA2 subfield of the dorsal hippocampus is essential for long-term spatial memory. *J. Neurosci.* **19,** 3535–3544
69. Hebert, A. E., and Dash, P. K. (2002) Extracellular signal-regulated kinase activity in the entorhinal cortex is necessary for long-term spatial memory. *Learn. Mem.* **9,** 156–166
70. Zhang, Z. G., Zhang, L., Jiang, Q., Zhang, R., Davies, K., Powers, C., Bruggen, N., and Chopp, M. (2000) VEGF enhances angiogenesis and promotes blood-brain barrier leakage in the ischemic brain. *J. Clin. Invest.* **106,** 829–838
71. Cheng, Y., Deshmukh, M., D'Costa, A., Demaro, J. A., Gidday, J. M., Shah, A., Sun, Y., Jacquin, M. F., Johnson, E. M., and Holtzman, D. M. (1998) Caspase inhibitor affords neuroprotection with delayed administration in a rat model of neonatal hypoxic-ischemic brain injury. *J. Clin. Invest.* **101,** 1992–1999
72. Schulz, J. B., Weller, M., and Moskowitz, M. A. (1999) Caspases as treatment targets in stroke and neurodegenerative diseases. *Ann. Neurol.* **45,** 421–429
73. Jin, K., Mao, X. O., Batteur, S. P., McEachron, E., Leahy, A., and Greenberg, D. A. (2001) Caspase-3 and the regulation of hypoxic neuronal death by vascular endothelial growth factor. *Neuroscience* **108,** 351–358
74. Guo, Y., Srinivasula, S. M., Druilhe, A., Fernandes-Alnemri, T., and Alnemri, E. S. (2002) Caspase-2 induces apoptosis by releasing proapoptotic proteins from mitochondria. *J. Biol. Chem.* **277,** 13430–13437
75. Bao, Q., and Shi, Y. (2007) Apoptosome. A platform for the activation of initiator caspases. *Cell Death Differ.* **14,** 56–65
76. Bouchier-Hayes, L., Oberst, A., McStay, G. P., Connell, S., Tait, S. W., Dillon, C. P., Flanagan, J. M., Beere, H. M., and Green, D. R. (2009) Characterization of cytoplasmic caspase-2 activation by induced proximity. *Mol. Cell* **35,** 830–840
77. Kumar, S. (2009) Caspase 2 in apoptosis, the DNA damage response and tumour suppression. Enigma no more? *Nat. Rev. Cancer* **9,** 897–903
78. Jin, K., Mao, X. O., Zhu, Y., and Greenberg, D. A. (2002) MEK and ERK protect hypoxic cortical neurons via phosphorylation of Bad. *J. Neurochem.* **80,** 119–125
79. National Institutes of Health (2011) *Guide for the Care of Use of Laboratory Animals*, NIH Publication 85-23, National Institutes of Health, Bethesda, MD